



OPEN ACCESS

EDITED BY

Arbind Kumar Patel,
Jawaharlal Nehru University, India

REVIEWED BY

Cristina Quintelas,
University of Minho, Portugal
Yanfu Wei,
Macau University of Science and
Technology, Macao SAR, China

*CORRESPONDENCE

María E. Peñafiel,
✉ maria.penafiel@ucuenca.edu.ec

RECEIVED 13 June 2023

ACCEPTED 24 July 2023

PUBLISHED 16 August 2023

CITATION

Jara-Cobos L, Abad-Delgado D,
Ponce-Montalvo J, Menendez M and
Peñafiel ME (2023), Removal of
ciprofloxacin from an aqueous medium
by adsorption on natural and
hydrolyzed bentonites.
Front. Environ. Sci. 11:1239754.
doi: 10.3389/fenvs.2023.1239754

COPYRIGHT

© 2023 Jara-Cobos, Abad-Delgado,
Ponce-Montalvo, Menendez and
Peñafiel. This is an open-access article
distributed under the terms of the
[Creative Commons Attribution License
\(CC BY\)](https://creativecommons.org/licenses/by/4.0/). The use, distribution or
reproduction in other forums is
permitted, provided the original author(s)
and the copyright owner(s) are credited
and that the original publication in this
journal is cited, in accordance with
accepted academic practice. No use,
distribution or reproduction is permitted
which does not comply with these terms.

Removal of ciprofloxacin from an aqueous medium by adsorption on natural and hydrolyzed bentonites

Lourdes Jara-Cobos¹, David Abad-Delgado¹,
Jonathan Ponce-Montalvo¹, Miguel Menendez² and
María E. Peñafiel^{1*}

¹Grupo de Ingeniería de las Reacciones Químicas, Catálisis y Tecnologías del Medio Ambiente (IRCMA), Departamento de Biociencias, Universidad de Cuenca, Ecocampus Balzay, Cuenca, Ecuador, ²Catalysis, Molecular Separations and Reactor Engineering Group (CREG), Aragon Institute of Engineering Research (I3A), Universidad Zaragoza, Zaragoza, Spain

Two bentonites (sodic bentonite, BSN, and calcic bentonite, BCN) were treated with nitric acid to improve the adsorption capacities using ciprofloxacin (CIP) as an adsorbate. The results demonstrated that nitric acid treatment enhances the specific area and increases the pore volume of both bentonites. The mechanism of adsorption of CIP was investigated using a kinetic model, isotherms, and pH influence. The adsorption capacity for BSN increased from 294.1 mg.g⁻¹ to 416.6 mg.g⁻¹ after acid treatment, while the increase in the adsorption capacity of BCN was minor. The increase in CIP removal may be due to an increase in the specific area and the presence of acidic surface functional groups. The adsorption mechanism of CIP on all adsorbents was governed by external diffusion, internal diffusion, and adsorption to reach equilibrium. The adjustment of strong adsorbents to the BET model indicated multilayer adsorption. The best adsorbent is sodic bentonite with nitric acid treatment. The study of the pH effect showed that the mechanism of CIP adsorption is hydrogen bonds and electrostatic interaction. Therefore, the acid treatment was found promising to improve the adsorbent characteristic of clays for removing CIP from water.

KEYWORDS

adsorption, ciprofloxacin, hydrolyzed bentonite, natural bentonite, removal

1 Introduction

Water is an invaluable natural resource to human beings and necessary for life on this planet. Many industrial processes and daily activities have caused water to be affected by the presence of pollutants. Among these, the so-called emerging pollutants (CEs) stand out, recognized for their presence in aquatic environments as pollutants of emerging concern (Krishnan et al., 2021), which include pharmaceuticals, dyes, endocrine disruptors, nanomaterials, flame retardants, artificial sweeteners, and personal care product ingredients (Correa-Sanchez and Peñuela, 2022; Gondi et al., 2022; Rigoletto et al., 2022). CEs generally come from treated or untreated wastewater that mixes with water from rivers, streams, groundwater, and marine environments (Peña-Álvarez and Castillo-Alanís, 2015). This is because they are not eliminated in

traditional treatment plants since they are not regulated and, thus, are not considered in their design, causing a global and growing problem since their constant release and lack of treatment could generate bioaccumulation, affecting human health and the environment (Gubitosa et al., 2022). The risk associated with the continued exposure of aquatic organisms to these contaminants in the environment is not only due to their acute toxicity but also due to their genotoxicity, their ability to develop resistance to pathogens, and the risk of endocrine disruption (Cuerda-Correa, 2019). Due to the aforementioned reasons, water contamination by the presence of CEs has become a serious environmental problem that requires urgent solutions based on pollution prevention, detection, and remediation (González-González et al., 2022).

Among the CEs, one of the groups that generate the greatest concern is antibiotics. The estimated consumption of antibiotics worldwide ranges between 1×10^5 and 2×10^5 tons per year, and recent studies indicate that in 2030, the global use of antibiotics will increase by 200% compared to that in 2015 (Haciosmanoğlu et al., 2022). Once consumed, antibiotics are partially metabolized in the body, with the remainder excreted via feces and urine (50%–80%) (Dutta and Mala, 2020); due to this, they were included in the European Union (EU) Watch List under the EU Water Framework Directive (Shamsudin et al., 2022). Ciprofloxacin (CIP) is one of the most widely used antibiotics. In the last 5 years, the consumption of oral ciprofloxacin has increased by 30% (Velusamy et al., 2021). Although ciprofloxacin is recognized to be hazardous to human health and the natural environment, its presence in watercourses and its disposal in wastewater are not effectively regulated (Shamsudin et al., 2022). Ciprofloxacin is known to be highly soluble in water (about 1.35 mg mL^{-1}) under different pH conditions and highly stable in wastewater and soil (Al-Jubouri et al., 2022). For this reason, the concentrations in which we find ciprofloxacin are in the range of 100 ng L^{-1} to $10 \text{ } \mu\text{g L}^{-1}$ in wastewater and from 100 to 500 mg L^{-1} in industrial and hospital effluents (Antonelli et al., 2020).

Several technologies have been tested to remove emerging contaminants; one of these technologies is advanced oxidation processes (AOPs), which are considered excellent for their effectiveness in removing various CEs. The main drawback of AOPs' current processes is that they are expensive since high-cost chemical products are used and consume high energy (Correa-Sanchez and Peñuela, 2022). Other processes, such as ozonation, require expensive equipment and could lead to the generation of bromate as a by-product, which is much more aggressive than the initial ones and has been shown to act as a carcinogen (Cuerda-Correa et al., 2019). According to those considerations, adsorption appears promising thanks to its efficiency and simple operation. It is a surface phenomenon widely recognized for its effective process for the removal of pollutants from wastewater. Its advantages are low cost, simple design, ease of wearing, and insensitivity to harmful substances (Rathi and Kumar 2021).

The cost related to the adsorption process depends mainly on the adsorbent used. Clays are considered potential alternative adsorbents due to their abundance, high specific surface area, low cost, and cation exchange capacity (Antonelli et al., 2020;

Leyva-Ramos et al., 2021). These clays, which are related to Miocene sedimentary lake basins, are considered environmentally friendly materials that do not present any environmental risk when used in wastewater treatment because they are obtained from natural sources (Biswas et al., 2019). The use of activated carbons and clays as adsorbent materials is almost as old as the adsorption technology for contaminant removal. Among the clays used, there are zeolites, bentonites, and kaolinites. Despite the dominant use of microporous activated carbons and other sophisticated adsorbent materials as nanomaterials, there is still a wide interest in the use of acid-modified clays, not only because of their abundance and low cost but also because the structure and dimension of their pores appear suitable compared to natural clays and organic residues. The latter has been used in recent years as low-cost adsorbents. The utilization of the different adsorbent materials is closely related to their surface properties, which depend on surface modification. Several methods have been suggested to improve the surface properties of clay, which include, among others, thermal modification, which reached a maximum adsorption capacity of 114.4 mg/g of CIP (Antonelli et al., 2020), and pillarization of clay to remove amoxicillin (Chauhan et al., 2020). Synthetic polymers and surfactants are also widely used for clay modification (Chen et al., 2023) (Sun et al., 2017). These methods are efficient but expensive, which can limit their use on a real scale. In Ecuador and other countries in Latin America, clays are abundant and low-cost materials used in the ceramic industry especially. However, their use for other purposes may be favorable. In addition, the main objective is to have a possible system using abundant and low-cost local materials for the removal of micropollutants. On the other hand, studies have shown that clayey materials are effective in removing emerging contaminants (Rizzi et al., 2020; Pérez-González et al., 2021; Roshanfekr Rad and Anbia, 2021; de Farias et al., 2022; Ortiz-Ramos et al., 2022). However, acid-modified clays have been poorly studied, especially with nitric acid.

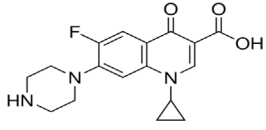
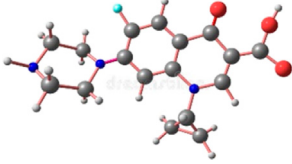
In this work, the behavior of CIP adsorption on natural and chemically modified sodium and calcium bentonite was studied and compared. The objective was to determine the best pH, kinetic, and equilibrium conditions for the application of these clays for the removal of the drug.

2 Materials and methods

Ciprofloxacin (CAS: 85721-33-1), $\geq 98\%$ HPLC grade, analytical grade supplied by Sigma-Aldrich, was used. Ciprofloxacin samples were prepared with 100 mg of ciprofloxacin in ultrapure water containing 1% methanol as a stock solution to a volume of 1,000 mL. The pH of the solutions was adjusted using HCl and 0.1 N NaOH, supplied by Merck. Table 1 shows the properties of ciprofloxacin.

Determination of ciprofloxacin concentrations was performed with a Thermo Scientific GENESYS™ 10S Ultraviolet-Visible Light (UV-Vis) Spectrophotometer. Measurements were made against a 1% methanol-water blank at a wavelength of 274 nm.

TABLE 1 Properties of ciprofloxacin.

Compound	Ciprofloxacin
Molecular formula	C ₁₇ H ₁₈ FN ₃ O ₃
Molecular weight (g.mol ⁻¹)	331.34
pH	3–4.5
Water solubility (mg.mL ⁻¹)	<1
2D structure	
3D structure	

2.1 Adsorbents

The sodium and calcium clay were obtained from the ECUAMINERAL Company. The cation exchange capacity is 202 meq.g⁻¹ and 70 meq.g⁻¹, respectively. These adsorbent materials were used in the adsorption process without any treatment and treated in an acid hydrolysis process using nitric acid (Sigma-Aldrich ACS reagent, 70%).

The acid treatment was carried out at a temperature of 90°C, and agitation was carried out for 3 h; filtration and washing were performed to eliminate acid residues, and, finally, they were dried in an oven at a temperature of 40°C for 24 h. A wide variety of acids are used for this reaction, the most common being HCl; however, its use should be avoided as it is a controlled-use reagent (Liu et al., 2013). According to Eggs, the chemical modification of rice hulls with phosphoric acid produced an increase in hexavalent chromium adsorption by approximately 100% (Eggs N. et al., 2012).

The materials were characterized by Brunauer–Emmett–Teller (BET) theory to determine the specific surface area of the clays using the Quantachrome QUADRASORB SI instrument. NOVA 2200 at a temperature of 77 K was used. Before starting the analysis, each of the samples was subjected to degassing at 300°C for 3 h to eliminate possible contaminants. The functional groups on the surface of the adsorbent materials used were determined by FTIR with the Nicolet IS5 FTIR spectrometer. The zero charge point of the adsorbents was determined using the methodology used by Antunes et al. (2012).

2.2 Adsorption test

Each test with each natural or treated adsorbent was carried out with variations in adsorbent weights, CPX solution concentrations, adsorption time, and pH value to determine the optimal process

conditions. All the tests were carried out in triplicate, and the average values are reported in this work.

The amount of adsorption q_e (mg.g⁻¹) of the samples was calculated by applying the following formula (El Azzouzi et al., 2022):

$$q_e = \frac{(C_o - C_e) \cdot V}{m} \quad (1)$$

The adsorption efficiency can be expressed as

$$\% R = \frac{C_o - C_e}{C_o} \times 100, \quad (2)$$

where C_o and C_e are the initial and equilibrium CIP concentrations (mg.L⁻¹), respectively. V is the volume of the solution (mL), and m is the mass of the adsorbent (mg).

2.3 Kinetic and equilibrium study

For the kinetic study, the experimental data obtained with a 20 mg.L⁻¹ CIP solution at times from 5 to 120 min were fitted to the kinetic models to investigate the adsorption mechanisms and possible rate-determining steps according to the pseudo first-order, pseudo second-order, and Weber and Morris models.

The pseudo first-order model is (Antonelli et al., 2020)

$$q = q_e(1 - e^{-k_1 t}), \quad (3)$$

where q , q_e are the amounts of CIP adsorbed (μmol.g⁻¹), t is the time (h), and k_1 is the rate constant (h⁻¹).

The pseudo second-order model is

$$\frac{q}{q_e} = \frac{k_2 q_e t}{1 + k_2 q_e t}, \quad (4)$$

where k_2 is the rate constant (g.μmol⁻¹.h⁻¹).

The intraparticle diffusion model (Weber and Morris model) is expressed by

$$q_t = K_d t^{0.5} + C, \quad (5)$$

where K_d is the constants of the intraparticle diffusion model (mg.g⁻¹ min^{1/2}) and C is the intersection of the graph with the vertical axis (mg.g⁻¹).

The experimental isotherms were adjusted to the Freundlich, Langmuir, BET, and Dubinin–Radushkevich (D–R) models.

The Freundlich model is (Chung et al., 2015)

$$q_e = k_f (C_e)^{1/n}, \quad (6)$$

where k_f is Freundlich's constant and n is the empirical constant indicating the type of adsorption isotherm.

The Langmuir model according to Chung is

$$q_e = \frac{q_{max} k_l C_e}{1 + k_l C_e}, \quad (7)$$

where q_{max} is the maximum amount of CIP adsorption related to monolayer formation and k_l is Langmuir's constant.

The BET model is (Foo and Hameed, 2010)

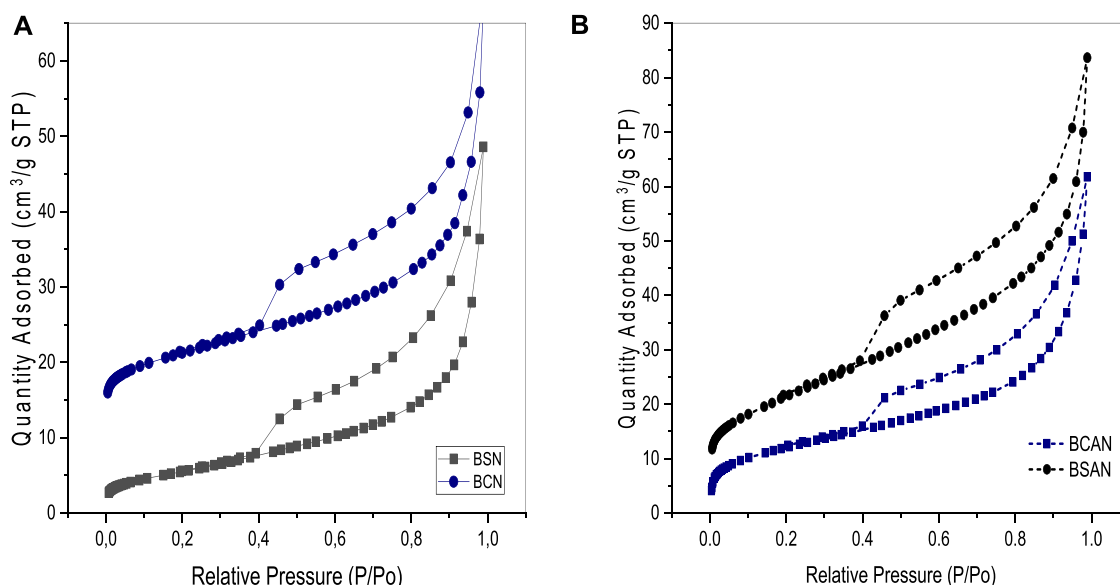


FIGURE 1 Adsorption isotherms. (A) Desorption of natural sodium bentonite and calcium bentonite. (B) Sodium and calcium bentonite treated with nitric acid.

$$\frac{C_e}{q_e(C_s - C_e)} = \frac{1}{q_s C_{BET}} + \frac{(C_{BET} - 1)}{q_s C_{BET}}, \tag{8}$$

where q_s is the theoretical adsorption capacity in the first layer ($\text{mg}\cdot\text{g}^{-1}$), C_s is monolayer saturation concentration ($\text{mg}\cdot\text{L}^{-1}$), and C_{BET} is the BET constant ($\text{L}\cdot\text{mg}^{-1}$).

The D-R model according to Foo (2010) is

$$\ln(q_e) = \ln(q_s) - K_{ad} \cdot \varepsilon^2, \tag{9}$$

$$E = \frac{1}{\sqrt{2K_{ad}}}, \tag{10}$$

where q_s is the maximum adsorption capacity ($\text{mg}\cdot\text{g}^{-1}$), K_{ad} is the activity coefficient related to the mean free energy of adsorption ($\text{mol}\cdot\text{kJ}^{-1}$), and ε is the Polanyi potential ($\text{kJ}\cdot\text{mol}^{-1}$). E is the average adsorption energy ($\text{kJ}\cdot\text{mol}^{-1}$).

2.4 Assessment of model fit

The obtained data were evaluated using the coefficient of determination (R^2) and the Marquardt percentage standard deviation (MPSD) (Foo and Hameed, 2010).

$$MPSD = \sqrt{\frac{1}{N-1} \sum_{i=1}^N \left(\frac{q_e - q_i}{q_e} \right)^2}. \tag{11}$$

3 Results and discussion

3.1 Characterization of adsorbents

The isotherms of natural sodium bentonite (BSN) and acid-treated sodium bentonite (BSAN), shown in Figure 1A, and the

isotherms of natural calcium bentonite (BCN) and acid-treated calcium bentonite (BCAN), shown in Figure 1B, belong to type IV in the Brunauer, Emmett, and Teller classification (Brunauer et al., 1938). This type of isotherm corresponds to porous or mesoporous solids and adsorption with multilayer formation and presents Langmuir adsorption isotherms (type I) in the region of low relative pressure, indicating the presence of micropores. Furthermore, the hysteresis loops of these isotherms are assigned to type H3 in the IUPAC classification, which is representative of slit-like pores in layered materials and is also related to the non-rigid nature of the adsorbent (Sing and Williams, 2004).

From Table 2, it can be observed that the surface area and pore volume increase with the acid treatment, while the pore size decreased 1.97 times for calcium bentonite and 2.51 times for sodium bentonite. It is an important indication that the modified clays will have improved properties and better adsorption capacity for wastewater treatment, as reported by Ding et al. (2008), for clays modified with acetic acid and hydrochloric acid. Activation of carbon by treatment with phosphoric acid favored the adsorption capacity due to its increase in surface area (Nguyen et al., 2023).

Table 3 shows the chemical composition of the natural sodium and calcium bentonites and their corresponding hydrolyzed forms in the percentage of oxides. A decrease in the content of some oxides is observed. However, the $\frac{\text{SiO}_2}{\text{Al}_2\text{O}_3}$ ratio increases in all cases, which may be due to impurities in the clay material (Sivrikaya et al., 2017). The acid treatment eliminates these impurities. Therefore, the values of this relationship decrease. An increase in the $\text{SiO}_2/(\text{Al}_2\text{O}_3 + \text{CaO} + \text{Na}_2\text{O} + \text{K}_2\text{O})$ ratio is also observed, indicating that the exchangeable cations have been replaced by H^+ cations (Díez et al., 2023).

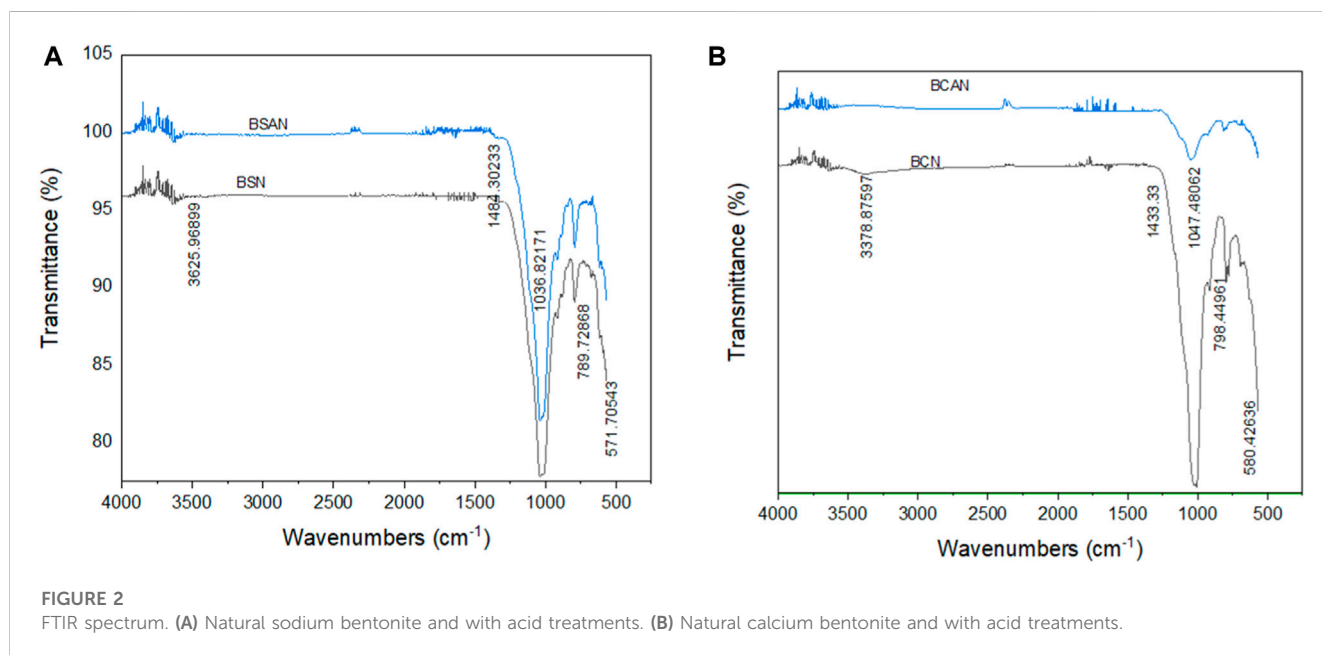
The adsorbents studied behave differently when balancing the pH. For natural calcium bentonite, the point of zero charge is 7.8, as shown in Table 2, while sodium bentonite has a much more basic point of zero charge (9.8). After the acid treatment, a decrease in the pH_{ZPC} was

TABLE 2 Surface area of natural and hydrolyzed bentonites.

Material	Specific surface $m^2.g^{-1}$	Pore volume $cm^3.g^{-1}$	Pore size nm	pH PCC
BCN	42	0.07	8.5	7.8
BSN	28	0.09	9.3	9.8
BSAN	70	0.32	3.7	4.7
BCAN	54	0.22	4.3	4.3

TABLE 3 Chemical composition of the natural and treated adsorbents.

	SiO ₂ %	Al ₂ O ₃ %	Fe ₂ O ₃ %	MgO %	CaO %	Na ₂ O %	K ₂ O %
BCN	60.50	17.59	6.22	1.05	2.84	1.00	1.25
BCAN	57.90	16.15	6.02	0.77	1.53	0.70	0.92
BSN	63.64	14.46	3.41	1.48	1.03	2.80	0.50
BSAN	63.61	14.33	2.93	0.90	0.27	0.72	0.45



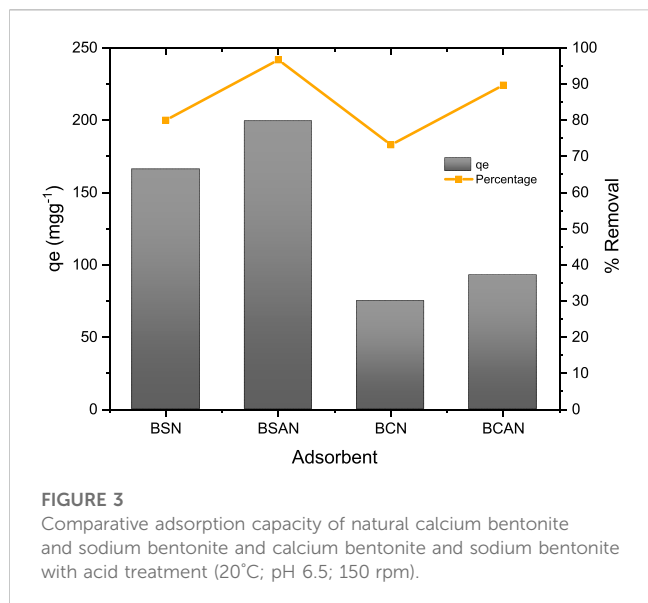
observed. The decrease in the point of zero charge would be due to the presence of a greater amount of H⁺. Other studies also demonstrated a decrease in the pH_{ZPC} value; e.g., rice husk and coconut shell decreased their zero charge point due to treatment with phosphoric acid (Eggs et al., 2012; Freddy and Anaguano, 2013).

The FTIR spectra of the clay samples, shown in Figure 2, were obtained from the mid-infrared region between 4,000 and 400 cm⁻¹. Most of the IR bands that appear in this region are due to mineral/inorganic substances (Pejčić et al., 2021). For calcium and sodium clays, both natural and treated, it can be seen that they present peaks between 1,250 and 950 cm⁻¹, which correspond to the Si–O–Si and Si–O–Al bond. According to Oye, the region between 1,100 and 650 cm⁻¹ is characterized

by the presence of Si–O bonds of silicates such as quartz and phyllosilicates (Oye, 2022). According to Kausar, it includes functional groups such as Al–Al–OH, C–H, and C–C stretching (Kausar et al., 2020). It can be seen that the spectra of the treated bentonites showed less-intense peaks than those of the corresponding original clays. The appearance of a peak at 1,370 cm⁻¹ may be due to treatment with nitric acid.

3.2 Adsorbent dose

The dose of each adsorbent was evaluated to achieve the maximum percentage of CIP adsorption. For this, 50 mL of a



20 mg.L⁻¹ CIP solution was shaken for 120 min at 20°C with different amounts of adsorbent in each test, and the range of weights used was 0.04–0.24 g.L⁻¹.

The percentage of drug removed with each adsorbent increases as the amount of adsorbent increases. This is because there is a greater number of active sites in which the drug is deposited. According to the results obtained, the maximum adsorption was related to a dose of 0.1 g.L⁻¹ for BSN and BSAN and 0.2 g.L⁻¹ for BCN and BCAN, as can be seen in [Supplementary Figure S2](#). These doses were used in all adsorption tests. This dose is less than necessary to reach the maximum percentage of adsorption of CIP on other adsorbents; for example, [Gulen et al. \(2020\)](#) used a dose of 2 g.L⁻¹ of montmorillonite, while [Peñafiel et al. \(2021\)](#) used a dose of 0.3 g.L⁻¹ for a commercial activated carbon and 3 g.L⁻¹ for sugarcane bagasse. [Yang et al. \(2022\)](#) used 2.5 g.L⁻¹ coconut fiber biochar.

The results show a greater CIP adsorption capacity in treated (BSAN) and natural (BSN) zeolites compared to BCAN and BCN. In addition, as observed in [Figure 3](#), the adsorption capacity in each case increases with the acid treatment, approximately by 20%. The adsorption capacity follows the order BSAN > BSN > BCAN > BCN. In addition, the percentage of adsorption increased from 78% to 99% with the acid treatment for sodium bentonite and from 72% to 90% with the treatment for calcium bentonite.

3.3 Contact time

Time is a very important factor in reaching equilibrium conditions. The effect caused by the exposure time of the adsorbent in the ciprofloxacin solution facilitates the determination of the adsorption efficiency and the equilibration time ([Aminu et al., 2020](#)).

For this study, the contact time varied from 5 to 120 min, using a 20 mg.L⁻¹ solution of CIP, at a pH of 6.5 and a stirring speed of 150 rpm, and the optimal doses for each adsorbent were used. The results are shown in [Figure 4](#).

The adjustment constants to the kinetic models are shown in [Table 4](#). The amount of CIP adsorbed by BSAN was 199 mg.g⁻¹ and 166 mg.g⁻¹ by BSN, both in 80 min. After that time, the amount adsorbed did not increase. Therefore, this time is considered the time necessary to reach equilibrium. BCN reached maximum adsorption of 75 mg.g⁻¹ in 60 min, while BCAN reached 92.5 mg.g⁻¹ in the same time. Adsorption on all adsorbents is rapid and is achieved in the first 10 min. The time to reach equilibrium is less than that found by [Bhadra et al. \(2017\)](#), 3 h, on a metal–organic framework and by [Hu et al. \(2019\)](#) when adsorbing CIP on a type of biochar.

The adsorption process in all natural and nitric acid-treated bentonites followed pseudo second-order kinetics since the coefficients of determination (R²) were close to 1. The linearized graphs of the pseudo second-order equation are shown in [Supplementary Figure S2](#). [Yang et al. \(2022\)](#) showed that the

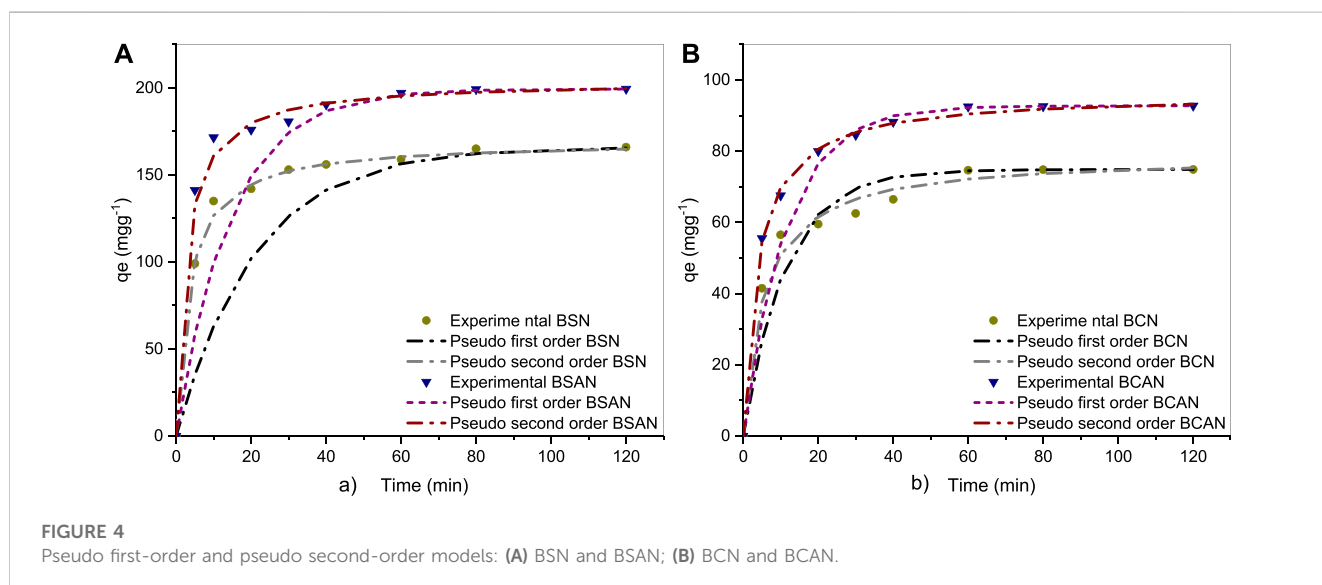
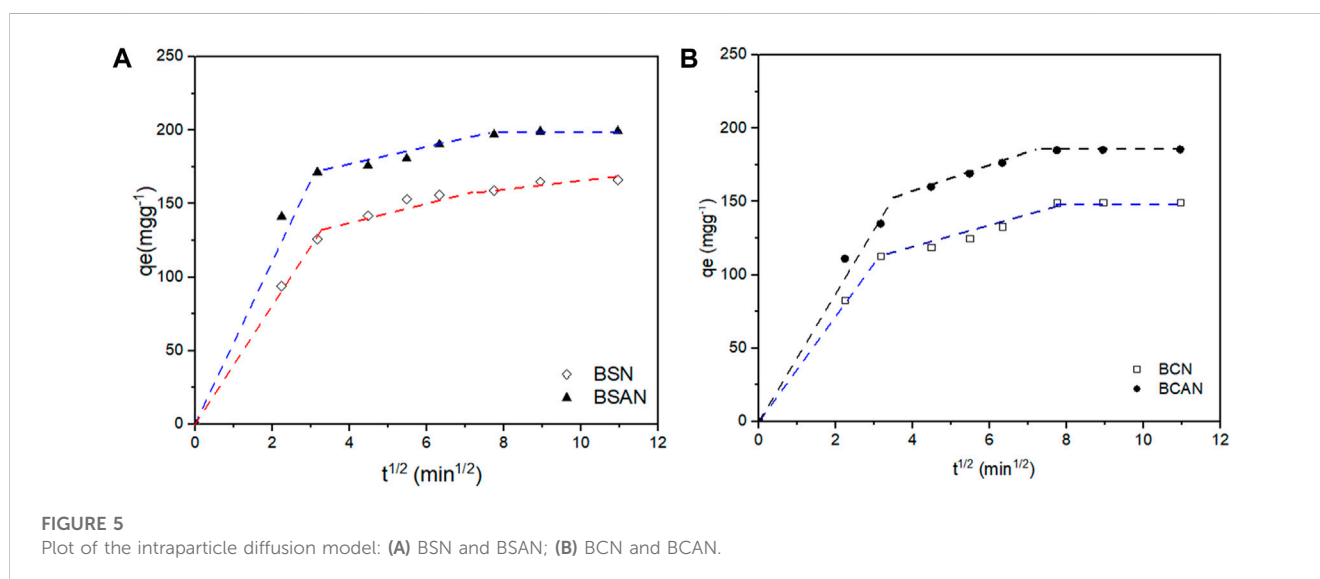


TABLE 4 Parameters of the pseudo first-order and pseudo second-order models.

Model	Parameters	BCN	BCAN	BSN	BSAN
Pseudo first order	q_e (SD) ($\text{mg}\cdot\text{g}^{-1}$)	74.8 (± 1.8)	92.7 (± 2.1)	166.0 (± 2.1)	199.4 (± 1.1)
	k_1 (min^{-1})	0.088	0.087	0.047	0.069
	R^2	0.91	0.95	0.93	0.94
Pseudo second order	q_e (SD) ($\text{mg}\cdot\text{g}^{-1}$)	78.4 (± 1.9)	96.1 (± 2.4)	169.5 (± 1.8)	204.0 (± 2.5)
	k_2 ($\text{g}\cdot\text{mg}^{-1}\cdot\text{min}^{-1}$)	0.002	0.002	0.002	0.002
	R^2	0.99	0.99	0.99	0.99



pseudo second-order model presents a better fit with the kinetic experimental data on the adsorption of CIP on coconut fiber. According to [Awad et al. \(2019\)](#), the adsorption kinetics predominantly follows the pseudo second-order model for natural and hydrolyzed clays.

The Weber and Morris intraparticle diffusion equation allows identifying the diffusion mechanisms involved in adsorption. [Figure 5](#) shows the graph of $t^{1/2}$ vs. q_e , and it can be seen that none of the intraparticle diffusion graphs passes through the origin; therefore, this is not the only stage that controls the adsorption process. All the graphs present three portions in the CIP adsorption, which indicates that there are three successive stages until equilibrium: 1) External diffusion, which in all cases is very fast and occurs in the first 10 min and where most of the adsorption occurs. 2) Internal diffusion or transport into the adsorbent particle. This process is longer; for BCN and BCAN, it was from 10 to 40 min, and it was from 10 to 60 min for BSN and BSAN. 3) Adsorption to reach saturation ([Kumar et al., 2011](#); [Suriyanon et al., 2013](#)).

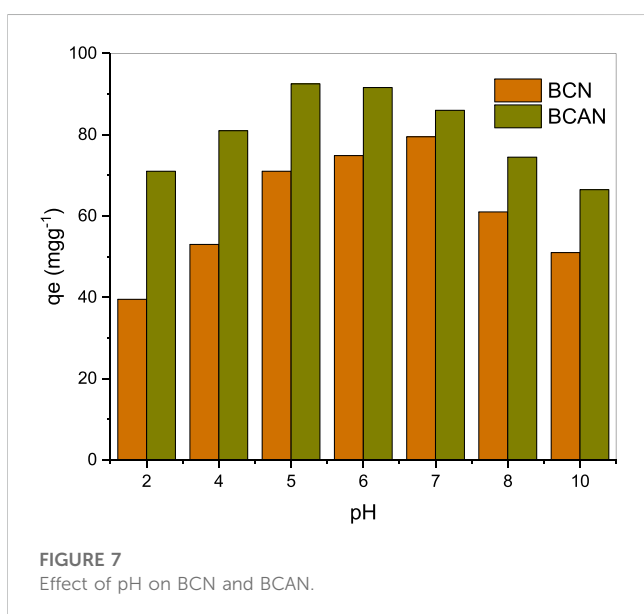
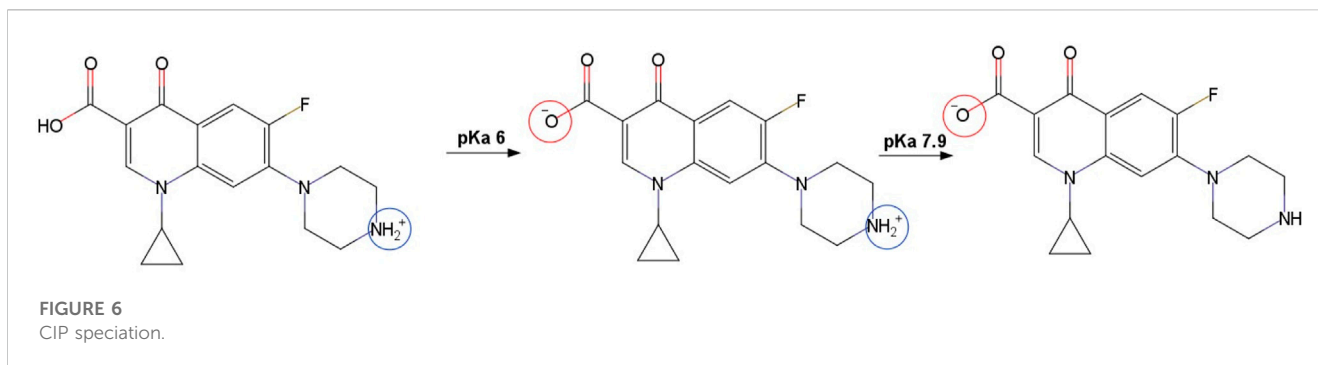
3.4 Effect of solution pH

The pH of the solution is one of the main factors influencing the adsorption process because the charge on the adsorbent

surface varies depending on the pH of the solution and its point of zero charge. In addition, it affects the charge of the functional groups of the adsorbent and their dissociation in the active sites of the same. Other properties that alter the pH are the solubility of the solution and its degree of ionization ([Khokhar et al., 2019](#)).

Ciprofloxacin is a zwitterionic molecule between its pKa values; that is, at values of pH 6 and pH 9, CIP ionizes positively and negatively. [Figure 6](#) shows the ionization of CIP.

The behavior of BCN and BCAN with the variation of the pH of the solution is shown in [Figure 7](#). BCN is neutral at pH_{PZC} 7.8, has a positive charge at lower values, and has a negative charge at higher pH values. At values less than 6, the CIP is cationic, so electrostatic repulsions decrease the amount of CIP adsorbed. At values greater than 8, both adsorbents and adsorbates have negative charges, which also favor repulsion. As with other adsorbents, CIP adsorbs better at pH values between 6 and 8 in its zwitterionic state. This may be because, at these pH values, the positive and negative charges of the CIP interact with the functional groups of the adsorbents, forming hydrogen bonds. The acid treatment decreases the pH_{PZC} in BCAN from 7.8 to 4.3 ([Table 2](#)). At pH values less than 4.3, both BCAN and CIP are positively charged and electrostatic repulsion influences adsorption. At pH 5, BCAN is negatively charged and CIP is positively charged, which causes an increase in CIP



adsorption compared to BCN. The same results were observed in CIP adsorption using BSN and BSAN.

The greater adsorption capacity of CIP shown by BSN over the adsorption capacity of BCN can be explained by the greater electrostatic attractions. BSN has a pH_{PZC} of 9.8, so any lower pH value will have a positive charge interacting with the CIP charges.

In addition to electrostatic interactions, there were other interactions between natural and treated bentonite and CIP. These mechanisms can be as follows:

- 1) The fluoride molecule contained in the CIP acts as an acceptor of the electrons (Al^+) present in natural and acid-treated bentonites. As seen in Table 4, the composition of natural bentonites changes with acid treatment. Principally, the reduction in Al_2O_3 content contributed to the leaching of Al^+ (Panda et al., 2010). The increase of Al^+ in the hydrolyzed bentonites increased the adsorption of CIP.
- 2) F and N molecules can form hydrogen bonds with O in bentonites. The increase in hydroxyl groups in bentonites after acid treatment increases the possibility of hydrogen bonding.
- 3) π - π interactions between Al and Si and aromatic ring in CIP.

- 4) Dipole interactions between the N in the amide group with acidic sites in bentonites (Chauhan et al., 2020).

Similar results were obtained in other studies. According to Akhtar, the amount of ciprofloxacin adsorbed on montmorillonite clay was almost constant for the pH range of 3–8 (Akhtar et al., 2016). Peñafiel et al. (2021) reported a maximum adsorption capacity at pH = 6 on sugarcane bagasse.

3.5 Adsorption studies

To obtain the equilibrium isotherms, different concentrations of the CIP solution (5 – 50 $mg \cdot L^{-1}$) were mixed with the optimal doses of each adsorbent and stirred at 150 rpm for 100 min at pH 6.5.

Figure 8 shows experimental isotherms comparing CIP adsorption on natural and acid-treated bentonites. Three isotherm models were used to fit the experimental data: Langmuir, Freundlich, and BET models. As observed in Figure 8, the experimental isotherms for the four adsorbents are type II, which correspond to multilayer physical adsorption. The relatively high R^2 values of the models suggest several adsorption mechanisms. The highest R^2 values were presented with the BET model, which will describe multilayer adsorption. According to the Freundlich model, adsorption is favorable in all cases with values of n greater than 1. The k_f value indicates the affinity of the adsorbate with the sorbent; the higher its value, the greater the affinity. The value of k_f is as follows: $BSAN > BSN > BCAN > BCN$. The values of the constants are shown in Table 5. According to the Langmuir model, the maximum adsorption capacity is achieved with BSAN of 416.6 $mg \cdot g^{-1}$, while BSN reached 294.1 $mg \cdot g^{-1}$, showing an increase of 1.4 times. However, the increase in adsorption capacity in BCN was from 164.0 to 175.4 $mg \cdot g^{-1}$, which did not show a significant increase. This result may be because Na has a greater exchange capacity than Ca (Won et al., 2023).

The adsorption energy (E) values, calculated by the D-R equation, were 8.6, 8.3, 8.5, and 8.1 $KJ \cdot mol^{-1}$ for BSAN, BSN, BCAN, and BCN, respectively. According to the D-R model, adsorption energy between 8 and 16 $KJ \cdot mol^{-1}$ shows an ionic exchange, while values less than 8 $KJ \cdot mol^{-1}$ indicate physical adsorption. The CIP adsorption values are close to 8 $KJ \cdot mol^{-1}$, indicating both physical adsorption and ion exchange.

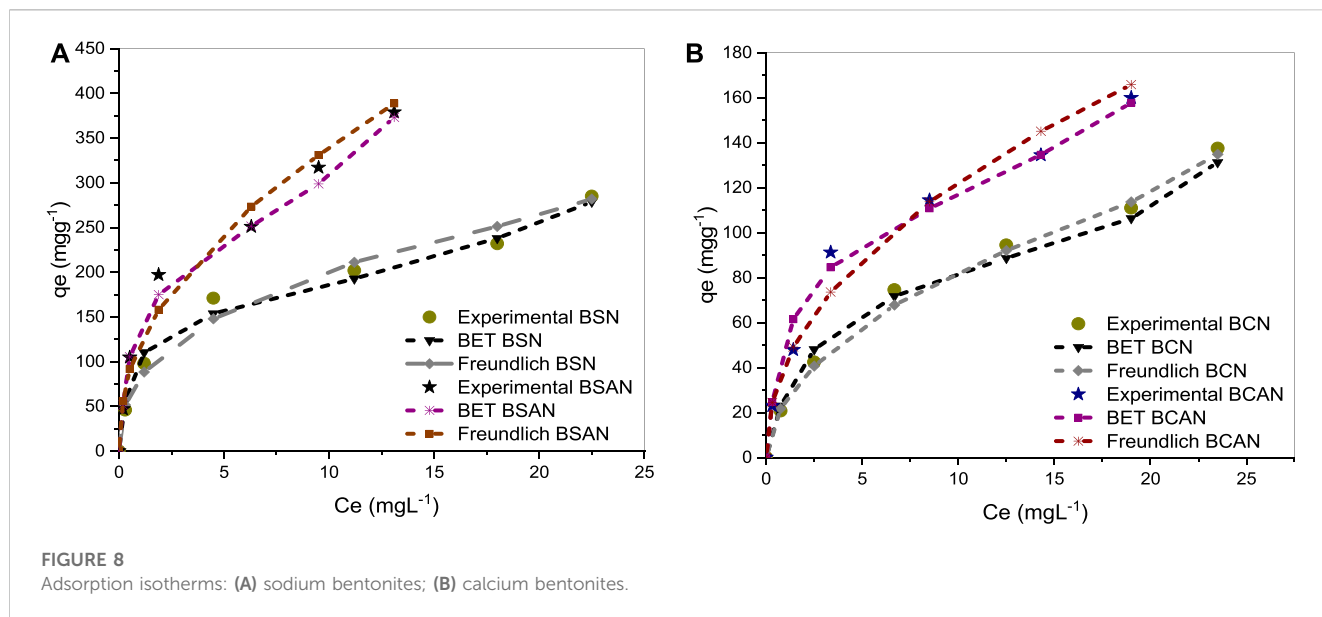


TABLE 5 Parameters of the adsorption models for the Langmuir, Freundlich, and BET isotherms.

Clays	Langmuir				Freundlich				BET			
	q_m	k_l	R ²	MPSD	k_f	n	R ²	MPSD	C_s	q_s	R ²	MPSD
	(mg·g ⁻¹)	(L·mg ⁻¹)			(mg/g) (mg/L) ^{-1/n}				(mg·L ⁻¹)	(mg·g ⁻¹)		
BSN	294.1 (±2.9)	0.352	0.96	12.3	82.2	2.1	0.98	10.5	40	154.2	0.99	4.1
BSNA	416.6 (±2.3)	0.462	0.96	15.5	117.9	2.5	0.97	8.6	30	225.2	0.99	8.2
BCN	164.0 (±2.3)	0.140	0.95	13.5	25.2	1.9	0.99	9.2	60	82.5	0.99	6.3
BCNA	175.4 (±2.1)	0.296	0.97	13.2	42.0	2.0	0.98	10.2	50	103.2	0.99	7.1

TABLE 6 Comparison of CIP adsorption capacities of various materials.

Adsorbents	q_{max} (mg·g ⁻¹)	S_{BET} (m ² ·g ⁻¹)	References
Natural sodium bentonite (BSN)	416.06	28	This studio
Sodium bentonite with nitric acid (BSAN)	294.1	70	
Natural calcium bentonite (BCN)	164.0	42	
Calcium bentonite with nitric acid (BCAN)	175.4	54	
Biochar with phosphoric acid activation	361.6	378.8	(Nguyen et al., 2023)
Thermally modified bentonite	114.4	1213.3	(Antonelli et al. (2020)
Seaweed biochar	270.0		(Nguyen et al., 2022)
Carbon activated by nanoparticles	109.8		(Al-Musawi et al., 2021)
Modified magnetic carbon	90.1	79.1	(Mao et al., 2016)
Commercial active carbon	78.1	643.9	(Peñafiel et al. (2021)
Pillared clay are Si and Fe	62.6	370	(Maggio et al., 2022)

Table 6 compares the adsorption capacities obtained in this study with others reviewed in the literature. The presented data show that the adsorption capacity of BSN and BSAN has satisfactory values in comparison with other adsorbents, such as activated carbons and nanomaterials. The results obtained show bentonites with acid treatment as efficient and possible adsorbent materials for pharmaceutical compounds. In addition, clays are abundant and much cheaper than other materials and are easily regenerable materials that allow desorption of contaminants and can be used several times in the adsorption process. Maget et al., 2020 tested five adsorption/desorption cycles with a mild solution of base and acid, decreasing the adsorption capacity between 10% and 40%.

4 Conclusion

This research found that natural bentonites (sodic and calcic bentonites) and nitric acid-treated bentonites effectively adsorbed the antibiotic ciprofloxacin. The specific area of bentonites increases with acid treatment. The results of the adsorption experiment showed that the adsorption of CIP was better on natural and treated sodic bentonite with acid treatment. The adsorption capacity was higher in sodium bentonite treated with nitric acid (416 mg.g^{-1}) than in natural sodium bentonite (294 mg.g^{-1}). Adsorption of CIP on all studied adsorbents is multilayer and could be affected by the initial pH solution. The experimental data adjusted better at the pseudo second-order kinetic model and the BET isotherm model. The Weber and Morris model showed three diffusion mechanisms in adsorption (Avci et al., 2020).

Data availability statement

The original contributions presented in the study are included in the article/Supplementary Material; further inquiries can be directed to the corresponding author.

References

- Akhtar, J., Nor Aishah, S. A., and Shahzad, K. (2016). A review on removal of pharmaceuticals from water by adsorption. *Desalination Water Treat.* 57 (27), 12842–12860. doi:10.1080/19443994.2015.1051121
- Aminu, I., Gumel, M., Ahmad, W. A., and Idris, A. A. (2020). Adsorption isotherms and kinetic studies of Congo-red removal from waste water using activated carbon prepared from jujube seed. *Am. J. Anal. Chem.* 11 (01), 47–59. doi:10.4236/ajac.2020.111004
- Antonelli, R., Geoffroy Roger, P. M., Gurgel Carlos da Silva, M., and Melissa Gurgel, A. V. (2020). Adsorption of ciprofloxacin onto thermally modified bentonite clay: Experimental design, characterization, and adsorbent regeneration. *J. Environ. Chem. Eng.* 8 (6), 104553. doi:10.1016/j.jece.2020.104553
- Antunes, M., Esteves, V. I., Guégan, R., Crespo, J. S., Fernandes, A. N., and Giovanela, M. (2012). Removal of diclofenac sodium from aqueous solution by isabel grape bagasse. *Chem. Eng. J.* 192 (June), 114–121. doi:10.1016/j.cej.2012.03.062
- Avci, A., İsmail, İ., and Baylan, N. (2020). Adsorption of ciprofloxacin hydrochloride on multiwall carbon nanotube. *J. Mol. Struct.* 1206 (April), 127711. doi:10.1016/j.molstruc.2020.127711
- Awad, A. M., Shaikh, S. M. R., Jalab, R., Gulied, M. H., Nasser, M. S., Benamor, A., et al. (2019). Adsorption of organic pollutants by natural and modified clays: A comprehensive review. *Sep. Purif. Technol.* 228 (December), 115719. doi:10.1016/j.seppur.2019.115719
- Azzouzi, E., Laila, S. E. A., Ennouhi, M., Ennouari, A., Kabbaj, O. K., and Zrineh, A. (2022). Removal of the amoxicillin antibiotic from aqueous matrices by means of an

Author contributions

Conceptualization: LJ-C and MP; methodology: LJ-C and MP; validation: MM; investigation: LJ-C, DA-D, and JP-M; writing—original draft preparation: LJ-C and MP; writing—review and editing: MP and MM; and supervision: MM. All authors contributed to the article and approved the submitted version.

Acknowledgments

The authors would like to acknowledge the Vicerrectorado de Investigación de la Universidad de Cuenca (VIUC).

Conflict of interest

The authors declare that the research was conducted in the absence of any commercial or financial relationships that could be construed as a potential conflict of interest.

Publisher's note

All claims expressed in this article are solely those of the authors and do not necessarily represent those of their affiliated organizations, or those of the publisher, the editors, and the reviewers. Any product that may be evaluated in this article, or claim that may be made by its manufacturer, is not guaranteed or endorsed by the publisher.

Supplementary material

The Supplementary Material for this article can be found online at: <https://www.frontiersin.org/articles/10.3389/fenvs.2023.1239754/full#supplementary-material>

adsorption process using kaolinite clay. *Sci. Afr.* 18 (November), e01390. doi:10.1016/j.sciaf.2022.e01390

BhadraNath, B., Ahmed, I., Kim, S., and SungJhung, H. (2017). Adsorptive removal of ibuprofen and diclofenac from water using metal-organic framework-derived porous carbon. *Chem. Eng. J.* 314 (April), 50–58. doi:10.1016/j.cej.2016.12.127

Biswas, B., Warr, L. N., Hilder, E. F., Goswami, N., Rahman, M. M., Churchman, J. G., et al. (2019). Biocompatible functionalisation of nanoclays for improved environmental remediation. *Chem. Soc. Rev.* 48 (14), 3740–3770. doi:10.1039/C8CS01019F

Bruna, S., Emmett, P. H., and Teller, E. (1938). Adsorption of gases in multimolecular layers. *J. Am. Chem. Soc.* 60 (2), 309–319. doi:10.1021/ja01269a023

Chauhan, M., Saini, V. K., and Suthar, S. (2020). Ti-pillared montmorillonite clay for adsorptive removal of amoxicillin, imipramine, diclofenac-sodium, and paracetamol from water. *J. Hazard. Mater.* 399, 122832. doi:10.1016/j.jhazmat.2020.122832

Chen, X., Tan, Y., Copeland, T., Chen, J., Peng, D., and Huang, T. (2023). Polymer elution and hydraulic conductivity of polymer-bentonite geosynthetic clay liners to bauxite liquors. *Appl. Clay Sci.* 242, 107039. doi:10.1016/j.clay.2023.107039

Chung, H. K., Kim, W. H., Park, J., Cho, J., Jeong, T. Y., and Park, P. K. (2015). Application of Langmuir and Freundlich isotherms to predict adsorbate removal efficiency or required amount of adsorbent. *J. Industrial Eng. Chem.* 28 (August), 241–246. doi:10.1016/j.jiec.2015.02.021

- Correa-Sanchez, S., and Peñuela, G. A. (2022). Peracetic acid-based advanced oxidation processes for the degradation of emerging pollutants: A critical review. *J. Water Process Eng.* 49 (October), 102986. doi:10.1016/j.jwpe.2022.102986
- Cuerda, C., Manuel, E., MaríaAlexandre-Franco, F., and Fernández-González, C. (2019). Advanced oxidation processes for the removal of antibiotics from water. An overview. *Water* 12 (1), 102. doi:10.3390/w12010102
- Díez, E., Redondo, C., José María, G., Miranda, R., and Rodríguez, A. (2023). Zeolite adsorbents for selective removal of Co(II) and Li(I) from aqueous solutions. *Water* 15 (2), 270. doi:10.3390/w15020270
- Ding, X., An, T., Li, G., Zhang, S., Chen, J., Yuan, J., et al. (2008). Preparation and characterization of hydrophobic TiO₂ pillared clay: The effect of acid hydrolysis catalyst and doped Pt amount on photocatalytic activity. *J. Colloid Interface Sci.* 320 (2), 501–507. doi:10.1016/j.jcis.2007.12.042
- Dutta, J., and Ahmad Mala, A. (2020). Removal of antibiotic from the water environment by the adsorption technologies: a review. *Water Science and Technology*, 82 401–426. doi:10.2166/wst.2020.335
- Eggs, N., Salvarezza, S., Azario, R., Fernández, N., and García, M. D. C. (2012). n.d. “Adsorción de Cromo hexavalente en La cáscara de Arroz modificada químicamente. *Julio-Sesptiembre* 3 (3), 141–151. Accessed January 31, 2023 <https://dialnet.unirioja.es/servlet/articulo?codigo=4052687>.
- Farias, M. D., Marcela, P. S., Lopes da Silva, T., Gurgel Carlos, D. S. M., and Melissa Gurgel, A V (2022). Natural and synthetic clay-based materials applied for the removal of emerging pollutants from aqueous medium. *Adv. Mater. Sustain. Environ. Remediat.* 359–92. Amsterdam, Netherlands Elsevier. doi:10.1016/B978-0-323-90485-8.00012-6
- Foo, K. Y., and Hameed, B. H. (2010). Insights into the modeling of adsorption isotherm systems. *Chem. Eng. J.* 156 (1), 2–10. doi:10.1016/j.ccej.2009.09.013
- Gondi, R., Kavitha, S., Kannah, R. Y., Karthikeyan, O. P., Kumar, G., Kumar Tyagi, V., et al. (2022). Algal-based system for removal of emerging pollutants from wastewater: A review. *Bioresour. Technol.* 344 (January), 126245. doi:10.1016/j.biortech.2021.126245
- González, G., Berenice, R., Flores-Contreras, E. A., Parra-Saldívar, R., Hafiz, M., and Iqbal, N. (2022). Bio-removal of emerging pollutants by advanced bioremediation techniques. *Environ. Res.* 214 (November), 113936. doi:10.1016/j.envres.2022.113936
- Gubitosa, J., Rizzi, V., Cignolo, D., Fini, P., Fanelli, F., and Cosma, P. (2022). From agricultural wastes to a resource: Kiwi peels, as long-lasting, recyclable adsorbent, to remove emerging pollutants from water. The case of ciprofloxacin removal. *Sustain. Chem. Pharm.* 29 (October), 100749. doi:10.1016/j.scp.2022.100749
- Gulen, B., and Demircivi, P. (2020). Adsorption properties of flouroquinolone type antibiotic ciprofloxacin into 2:1 dioctahedral clay structure: Box-behnken experimental design. *J. Mol. Struct.* 1206 (April), 127659. doi:10.1016/j.molstruc.2019.127659
- Haciosmanoğlu, G. G., Mejias, C., Martín, J., Santos, J. L., Aparicio, I., and Alonso, E. (2022). Antibiotic adsorption by natural and modified clay minerals as designer adsorbents for wastewater treatment: A comprehensive review. *J. Environ. Manag.* 317, 115397. doi:10.1016/j.jenvman.2022.115397
- Hu, Y., Zhu, Y., Zhang, Y., Tang, L., Zeng, G., Zhang, S., et al. (2019). An efficient adsorbent: Simultaneous activated and magnetic ZnO doped biochar derived from camphor leaves for ciprofloxacin adsorption. *Bioresour. Technol.* 288 (September), 121511. doi:10.1016/j.biortech.2019.121511
- Kausar, A., Sher, F., Abu, H., Javed, A., Sillanpää, M., and Iqbal, M. R. (2020). Biocomposite of sodium-alginate with acidified clay for wastewater treatment: Kinetic, equilibrium and thermodynamic studies. *Int. J. Biol. Macromol.* 161 (October), 1272–1285. doi:10.1016/j.ijbiomac.2020.05.266
- Khokhar, T. S., Memon, F. N., Ali Memon, A., Durmaz, F., Memon, S., Khan Panhwar, Q., et al. (2019). Removal of ciprofloxacin from aqueous solution using wheat bran as adsorbent. *Sep. Sci. Technol.* 54 (8), 1278–1288. doi:10.1080/01496395.2018.1536150
- Krishnan, R. Y., Manikandan, S., Subbaiya, R., Biruntha, M., Govarthanan, M., and Karmegam, N. (2021). Removal of emerging micropollutants originating from pharmaceuticals and personal care products (PPCPs) in water and wastewater by advanced oxidation processes: A review. *Environ. Technol. Innovation* 23 (August), 101751. doi:10.1016/j.eti.2021.101751
- Kumar, D., and Gaur, J. P. (2011). Chemical reaction- and particle diffusion-based kinetic modeling of metal biosorption by a phormidium sp.-dominated cyanobacterial mat. *Bioresour. Technol.* 102 (2), 633–640. doi:10.1016/j.biortech.2010.08.014
- Jubouri, A., Sama, M., Al-Jendeel, H. A., Rashid, S. A., and Al-Batty, S. (2022). Antibiotics adsorption from contaminated water by composites of ZSM-5 zeolite nanocrystals coated carbon. *J. Water Process Eng.* 47 (June), 102745. doi:10.1016/j.jwpe.2022.102745
- Leyva, R., Robertojacobó-Azuara, A., and Jesus Ivan Martínez, C. (2021). “Organoclays. Fundamentals and applications for removing toxic pollutants from water solution,” in *Porous materials, edited by Juan Carlos Moreno-piraján, Liliana giraldo-gutierrez, and fernando gómez-granados*, 341–63. *Engineering materials* Berlin, Germany (Cham Springer International Publishing). doi:10.1007/978-3-030-65991-2_13
- Liu, H., Peng, Y., Qin, Z., Dong, L., Tan, D., Zhu, J., et al. (2013). Thermal degradation of organic matter in the interlayer clay-organic complex: A TG-FTIR study on a montmorillonite/12-aminolauric acid system. *Appl. Clay Sci.* 80 (August), 398–406. doi:10.1016/j.clay.2013.07.005
- Maged, A., Kharbush, S., Ismael, I. S., and Bhatnagar, A. (2020). Characterization of activated bentonite clay mineral and the mechanisms underlying its sorption for ciprofloxacin from aqueous solution. *Environ. Sci. Pollut. Res.* 27, 32980–32997. doi:10.1007/s11356-020-09267-1
- Maggio, A. A., Maria, E. R. J., Villarrol-Rocha, J., Sapag, K., and Baschini, M. T. (2022). Fe- and SiFe-pillared clays from a mineralogical waste as adsorbents of ciprofloxacin from water. *Appl. Clay Sci.* 220 (April), 106458. doi:10.1016/j.clay.2022.106458
- Mao, H., Wang, S., Lin, J. Y., Wang, Z., and Ren, J. (2016). Modification of a magnetic carbon composite for ciprofloxacin adsorption. *J. Environ. Sci.* 49 (November), 179–188. doi:10.1016/j.jes.2016.05.048
- Musawi, A., Tariq, J., Amir Hossein, M., Aram Dokht, K., and Balarak, D. (2021). Effective adsorption of ciprofloxacin antibiotic using powdered activated carbon magnetized by iron(III) oxide magnetic nanoparticles. *J. Porous Mater.* 28 (3), 835–852. doi:10.1007/s10934-021-01039-7
- Nguyen, T. B., Quoc-Minh, T., Chen, C. W., Chen, W. H., and Cheng, D. D. (2022). Pyrolysis of marine algae for biochar production for adsorption of ciprofloxacin from aqueous solutions. *Bioresour. Technol.* 351 (May), 127043. doi:10.1016/j.biortech.2022.127043
- Nguyen, T. K., Nguyen, T. B., Chen, W. H., Chen, C. W., Bui, A. K. P. T., Chen, L., et al. (2023). Phosphoric acid-activated biochar derived from sunflower seed husk: Selective antibiotic adsorption behavior and mechanism. *Bioresour. Technol.* 371 (March), 128593. doi:10.1016/j.biortech.2023.128593
- Ortiz-Ramos, U., Leyva-Ramos, R., Mendoza-Mendoza, E., and Aragón-Piña, A. (2022). Removal of tetracycline from aqueous solutions by adsorption on raw Ca-bentonite. Effect of operating conditions and adsorption mechanism. *Chem. Eng. J.* 432 (March), 134428. doi:10.1016/j.ccej.2021.134428
- Oye, O. J. (2022). Integrated reflection-FTIR and multivariate partial least squares approach for rapid and accurate assessment of total organic carbon concentration in shale. *J. Petroleum Sci. Eng.* 217 (October), 110912. doi:10.1016/j.petrol.2022.110912
- Panda, A. K., Mishra, B. G., Mishra, D. K., and Singh, R. K. (2010). Effect of sulphuric acid treatment on the physico-chemical characteristics of kaolin clay. *Colloids surfaces A Physicochem. Eng. aspects* 363 (1–3), 98–104. doi:10.1016/j.colsurfa.2010.04.022
- Pejčić, B., Heath, C., Pagès, A., and Leon, N. (2021). Analysis of carbonaceous materials in shales using mid-infrared spectroscopy. *Vib. Spectrosc.* 112 (January), 103186. doi:10.1016/j.vibspec.2020.103186
- Peña-Álvarez, A., and Castillo-Alanís, A. (2015). Identificación y cuantificación de contaminantes emergentes en aguas residuales por microextracción en fase sólida-cromatografía de gases-espectrometría de masas (MEFS-CG-EM). *TIP* 18 (1), 29–42. doi:10.1016/j.recqb.2015.05.003
- Peñafiel, M. E., Matesanz, J. M., Vanegas, E., Bermejo, D., Mosteo, R., and Ormad, M. P. (2021). Comparative adsorption of ciprofloxacin on sugarcane bagasse from Ecuador and on commercial powdered activated carbon. *Sci. Total Environ.* 750 (January), 141498. doi:10.1016/j.scitotenv.2020.141498
- Pérez-González, A., Pinos-Vélez, V., Cipriani-Avila, I., Capparelli, M., Jara-Negrete, E., Alvarado, A., et al. (2021). Adsorption of estradiol by natural clays and Daphnia magna as biological filter in an aqueous mixture with emerging contaminants. *Eng* 2 (3), 312–324. doi:10.3390/eng2030020
- Rad, R., Leilaand Anbia, M. (2021). Zeolite-based composites for the adsorption of toxic matters from water: A review. *J. Environ. Chem. Eng.* 9 (5), 106088. doi:10.1016/j.jece.2021.106088
- Rathi, B. S., and Senthil Kumar, P. (2021). Application of adsorption process for effective removal of emerging contaminants from water and wastewater. *Environ. Pollut.* 280 (July), 116995. doi:10.1016/j.envpol.2021.116995
- Rigoletto, M., Calza, P., Gaggero, E., and Laurenti, E. (2022). Hybrid materials for the removal of emerging pollutants in water: Classification, synthesis, and properties. *Chem. Eng. J. Adv.* 10 (May), 100252. doi:10.1016/j.cjea.2022.100252
- Rizzi, V., Gubitosa, J., Fini, P., Romita, R., Agostiano, A., Nuzzo, S., et al. (2020). Commercial bentonite clay as low-cost and recyclable ‘natural’ adsorbent for the carbendazim removal/recover from water: Overview on the adsorption process and preliminary photodegradation considerations. *Colloids Surfaces A Physicochem. Eng. Aspects* 602 (October), 125060. doi:10.1016/j.colsurfa.2020.125060
- Shamsudin, M. S., Syahida, F. A., and Ismail, S. (2022). A review of diclofenac occurrences, toxicology, and potential adsorption of clay-based materials with surfactant modifier. *J. Environ. Chem. Eng.* 10 (3), 107541. doi:10.1016/j.jece.2022.107541
- Sing, K. S. W., and Williams, R. T. (2004). Physisorption hysteresis loops and the characterization of nanoporous materials. *Adsorpt. Sci. Technol.* 22 (10), 773–782. doi:10.1260/0263617053499032
- Sivrikaya, O., Uzal, B., and Ozturk, Y. E. (2017). Practical charts to identify the predominant clay mineral based on oxide composition of clayey soils. *Appl. Clay Sci.* 135 (January), 532–537. doi:10.1016/j.clay.2016.09.035

- Sun, K., Shi, Y., Wang, X., and Li, Z. (2017). Sorption and retention of diclofenac on zeolite in the presence of cationic surfactant. *J. hazardous mater.* 323, 584–592. doi:10.1016/j.jhazmat.2016.08.026
- Suriyanon, N., Punyapalakul, P., and Ngamcharussrivichai, C. (2013). Mechanistic study of diclofenac and carbamazepine adsorption on functionalized silica-based porous materials. *Chem. Eng. J.* 214 (January), 208–218. doi:10.1016/j.cej.2012.10.052
- Velusamy, K., Periyasamy, S., Senthil Kumar, P., Jayaraj, T., Krishnasamy, R., Sindhu, J., et al. (2021). Analysis on the removal of emerging contaminant from aqueous solution using biochar derived from soap nut seeds. *Environ. Pollut.* 287 (October), 117632. doi:10.1016/j.envpol.2021.117632
- Villa, A. F., and Anaguano, A. (2013). Determinación del punto de Carga cero y el punto isoeléctrico de Dos residuos agrícolas y su aplicación en La eliminación de Colorantes. *RIAA* 4 27-36. <https://dialnet.unirioja.es/servlet/articulo?codigo=5344979>.
- Won, J., Kim, J. U., and Choo, H. (2023). Estimation of the swelling strain and swelling pressure of compacted bentonite using electrical conductivity. *Appl. Clay Sci.* 242, 107040. doi:10.1016/j.clay.2023.107040
- Yang, Y., Luo, X., Zhang, J., Ma, X., Sun, P., and Zhao, L. (2022). Sewage sludge-coconut fiber Co-pyrolysis biochar: Mechanisms underlying synergistic heavy metal stabilization and ciprofloxacin adsorption. *J. Clean. Prod.* 375 (November), 134149. doi:10.1016/j.jclepro.2022.134149